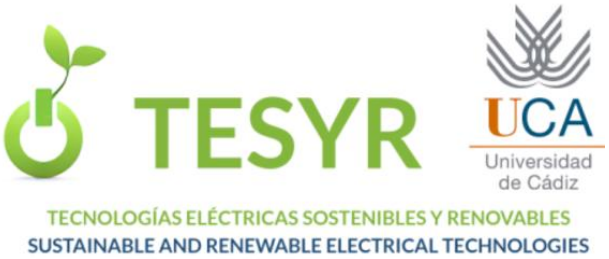

Control of an Hybrid AC/DC MG Using Raspberry

Carrasco González, David; Sarrias Mena, Raúl; Horrillo Quintero, Pablo; Llorens Iborra, Francisco; Fernández Ramírez, Luis Miguel

Published in:
SPRINGER NATURE Link

DOI (link to publication from Publisher):
https://doi.org/10.1007/978-3-031-73921-7

Publication date:
2025

Document Version:
Camera ready

Control of an Hybrid AC/DC MG Using Raspberry Pi

David Carrasco-González · Raúl Sarrias-Mena · Pablo Horrillo-Quintero · Francisco Llorens-Iborra · Luis M. Fernández-Ramírez

Abstract Nowadays, hybrid AC/DC microgrids (HMG) are growing in popularity because of human needs and their benefits. They are composed of the interconnection of a DC microgrid (MG) and an AC MG, and each MG is constituted by generation, energy storage, and consumption technologies. This study develops a new control strategy for an HMG consisting of a DC MG and an AC MG interconnected through a bidirectional power converter. The AC MG is composed of AC loads, a photovoltaic (PV) generator and a battery bank. The DC MG is made up of a hydrogen system, DC loads, wind turbine (WT) and ultracapacitor (UC). The HMG is evaluated under different conditions in an experimental setup constituted by an OPAL-RT 4512 unit and a Raspberry Pi microcontroller. This experimental setup permits to execute the HMG in real time and to validate the results obtained. Finally, the control system developed for this HMG presents a satisfactory behaviour under different working conditions.

1 Introduction

Currently, the employment of renewable power sources in power generation has emerged incredibly important because of international initiatives to mitigate climate change by diminishing greenhouse gas pollutants and phasing out fossil fuels, and this type of energy sources offers a convenient solution to this challenge [1]. On the other hand, there is an exponential growth in cities and industries that generates a higher power demand. Hence, these matters create a demand for the transformation of traditional power grids into autonomous and small-scale grids, denominated as microgrids (MGs). MGs are attractive solutions due to their numerous benefits, including reduced carbon emissions, cost-effective operation, enhanced power reliability and quality and higher energy efficiency [2].

MGs are controllable and cohesive systems that integrates a variety of energy storage systems (ESSs), renewable energy technologies (RETs), and distributed loads. They operate within specified electrical limits and function as integrated units [3]. The compatibility among AC MGs and conventional grids has generated considerable interest in their investigation. However, in recent years, there has been a surge in attention towards DC MGs [4]. Consequently, MGs can be operated using DC, AC, or a combination of DC/AC technologies, providing more adaptability and flexibility [5].

As the MGs can be self-sufficient, they can be isolated and located in remote areas without communication with a main grid [6]. However, this is not the typical situation of MGs and they are commonly interconnected to a main grid through a point of common coupling (PCC), which permits the MG to operate in two different states: a) grid-connected state, where the power imbalances of the MG are absorbed and supplied by the main grid [7]; and b) islanded state, where the energy generated in the MG can only be consumed or stored [8].

The concept of the integration of DC/AC technologies and the connection of a MG to the main grid produce the idea of interconnecting an AC MG and a DC MG to constitute a hybrid AC/DC microgrid (HMG) [9]. An HMG is managed

D. Carrasco-González · P. Horrillo-Quintero · F. Llorens-Iborra · L. M. Fernández-Ramírez
SURET Research Group, Department of Electrical Engineering, University of Cadiz (UCA)
ETSI Algeciras, Avda. Ramón Puyol, s/n
11202 Algeciras, Cadiz, Spain
e-mail: david.carrasco@uca.es, pablo.horrillo@uca.es, francisco.llorens@uca.es, luis.fernandez@uca.es

R. Sarrias-Mena
SURET Research Group, Department of Engineering in Automation, Electronics and Computer Architecture and Networks, University of Cadiz (UCA)
ETSI Algeciras, Avda. Ramón Puyol, s/n
11202 Algeciras, Cadiz, Spain
e-mail: raul.sarrias@uca.es

cooperatively to achieve its objectives and offers the benefits of independent DC and AC MGs. Furthermore, HMG offers enhanced reliability, efficiency, and the ability to integrate diverse power sources [10].

In this context, MGs are managed employing energy management systems (EMSs) to reach their objectives. The main purpose of the EMS is to provide the references to the energy sources that constitute the MG, and this can be accomplished through various methods [11], [12].

This study introduces a new control strategy for an HMG composed of a DC MG and an AC MG connected to a main grid. This system is implemented into an experimental setup to validate the results. The experimental setup is composed of a Raspberry Pi microcontroller integrated into a real communication network, a real-time emulated HMG executing on an OPAL RT-4512 unit, and a PC host.

In this study, Section 2 provides a comprehensive overview of the HMG and control strategy. The experimental setup of the HMG is developed in Section 3. In Section 4, the experimental results are illustrated and analysed. In the final Section (Section 5), the conclusions of this study are presented.

2 Configuration and Control of the Hybrid AC/DC Microgrid

Fig. 1 illustrates the HMG examined in this study, which is constituted by a DC MG interconnected to an AC MG via a voltage source inverter. In addition, this last MG is connected to a main grid, specifically a stiff three-phase AC grid.

The control strategy addresses two important actions. The first one is that all the components of each MG are independently and individually controlled to comply with a specific reference. In the second one, the EMS acts as centralized control coordinating the operation of all the components of the HMG. In the remainder of this section, a detailed description of the control systems and the MGs is presented.

2.1. DC Microgrid

The DC MG is constituted by an UC, WT, DC loads, and a hydrogen system (fuel cell plus electrolyzer) interconnected to a common DC bus, as presented in Fig. 1.

A synchronous generator, which is modelled as a sixth-order system, is considered for the WT. This generator is interconnected to the DC bus via an uncontrolled bridge rectifier and a DC boost converter. The first one transforms the AC output of the WT into DC power. The converter regulates the speed of the WT to achieve optimal operation in response to varying wind speed.

In terms of the ESSs, the fuel cell (FC) is emulated using a controlled voltage source plus one diode model. The electrolyzer (EZ) is emulated using a voltage source with a series resistor. Finally, the UC is modelled by an ideal capacitor with a series resistor. These systems are interconnected to the DC MG in various ways: a boost converter is employed for the FC, a buck converter is utilized for the EZ, and a bidirectional half-bridge converter, implemented with IGBTs, is used for the UC. The election of each converter is due to the direction of energy exchange in each system.

The DC loads in this MG are directly coupled to the DC bus via a circuit breaker for each load to interrupt or establish the connection of these loads.

Lastly, the VSI is utilized to connect the DC bus of this MG to the AC bus of the AC MG. The essential purpose of this converter is to regulate and stabilize the DC bus voltage,

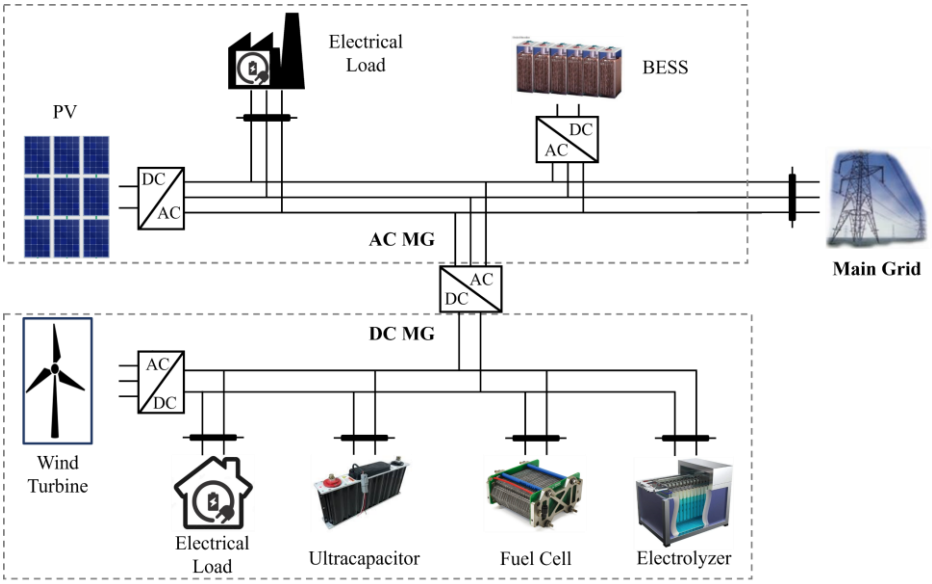

Fig. 1. Configuration of the HMG.

ensuring it maintains constant despite power fluctuations derived from the variable wind speeds and load changes. Additionally, this VSI allows to convert the DC power to AC power of the grid [13].

2.2. AC Microgrid

The AC MG is constituted by AC loads, battery ESS (BESS), and PV generator. This MG is interconnected to the main grid via the PCC, as illustrated in Fig. 1.

In this study, the PV panels are modelled utilizing a combination of a common current source, a parallel diode model, and a series and parallel resistor [14]. These PV panels are interconnected to the AC bus via a boost converter and a VSI. The boost converter allows to raise the voltage and implement the maximum power point tracking (MPPT) technique for the PV panels. The MPPT strategy uses the perturb and observe (P&O) algorithm to determine the duty cycle of the boost converter. Alternatively, the VSI regulates the voltage and frequency to guarantee the compatibility of the DC power with the AC bus, using a cascaded control loop based on PI regulators.

The BESS is a Li-ion BESS, emulated as a controlled voltage source plus series resistors. The BESS is interconnected to the AC MG employing a VSI, which is controlled to adjust the active and reactive power exchange of the BESS and the rest of the system utilizing a cascaded control loop.

Finally, the AC loads are two three-phase constant RL loads, in a star arrangement. To observe the response of the control strategy of the HMG, they are connected and disconnected from the AC MG at various time intervals.

2.3. Main Grid

The HMG is connected to the main grid, that is implemented with a stiff three-phase AC grid. The grid is modelled as an ideal three-phase AC voltage source with constant voltage and frequency. In this paper, the HMG operates in the grid-connected state.

Because the frequency and voltage are self-regulated by the main grid, it does not require any control action. Additionally, the active and reactive power exchanges are also self-regulated to guarantee the power balance and avoid frequency and voltage deviations.

2.4. Local control

This subsection summarizes the local controls implemented in each component of the HMG. For the WT, its speed is regulated to follow the optimal power curve under variable wind speed. In the PV generator, the solar radiation is also a variable parameter, and hence, the MPPT strategy is employed to optimize the energy generation.
To ensure in the UC, hydrogen system, and BESS that the active power exchange follows the references supplied by the EMS, PI regulators are employed. As the BESS and the UC can be charged and discharged, negative and positive active power references are possible. Otherwise, the FC can only receive positive values and the EZ negative values.

Lastly, DC and AC loads do not require any control strategy and only their disconnection and connection are managed by means of a time-controlled circuit breaker.

2.5. Centralized control

In this study, the centralized control is an EMS that realizes the cooperative operation of the HMG, managing the energy exchange between all the elements and ensuring that the loads demand is supplied.

In the EMS, the DC and AC loads constitute a unique demand pool, and the PV generator and WT constitute a unique generation pool. When there is a power imbalance in the HMG, the ESSs cover this mismatch according to the characteristic of each ESS. In this context, the BESS is the preferred ESS for the power regulation, while its state of charge (SOC) is monitored to prevent excessively low or high SOC conditions. The hydrogen system assists in maintaining the SOC level and each component is kept to a minimum consumption or generation regime to avoid their disconnection of the system. Lastly, the objective of the UC is to address rapid and temporary power mismatches caused by the slower response of the hydrogen system and the BESS.

Following these premises, the generated and demanded energy are compared. If demand is higher than generation, the ESSs will have to contribute to this energy deficit, and vice versa when generation is higher than demand. After this stage, to determine whether the BESS is capable of releasing/storing energy, its SOC is evaluated. When the SOC falls within a ‘LOW’ range, it can no longer be discharged, and the FC provides the additional power needed to meet the power mismatch. In the opposite range, when the SOC is ‘HIGH’, the EZ is used to absorb excess energy because the BESS cannot absorb anymore. In the middle range, when the SOC is among ‘LOW’ and ‘HIGH’, the hydrogen system and the BESS are employed to cover power mismatch in the HMG. Finally, in the last stage, the active power reference of the UC is computed by calculating the variation among the active power measured of the FC, the BESS, and the EZ and their reference values. As previous mentioned, the objective of the UC is to cover the power imbalance during transitory intervals owing to its quick response.

Lastly, if the ESSs cannot cover the power mismatches, owing to the capacity, speed or power constrains, the main grid will respond to solve this imbalance.

3 Experimental Setup

This section details the experimental setup utilized to implement the proposed HMG and it is structured as follow: Subsection 3.1 describes the structure of the experimental

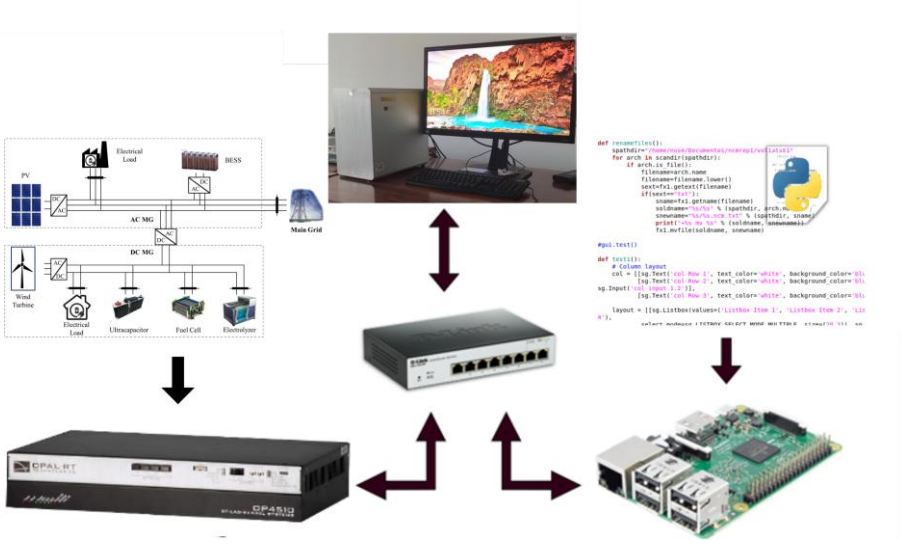

Fig. 2. Experimental setup.

setup, and Subsection 3.2 explains the communication link protocol run in this experimental setup.

3.1. Structure of the Experimental Setup

The experimental setup consists of an OPAL-RT 4512 real time simulator unit, a Raspberry Pi microcontroller, and a PC host, as illustrated in Fig. 2.

OPAL-RT is a real-time simulator of hardware-in-the-loop (HIL) test systems which enables the implementation of MATLAB/Simulink models. In this study, an OPAL-RT 4512 unit is programmed employing RT-LAB software, which permits editing, building, loading, executing and monitoring of models. This combination facilitates a high-performance in a real-time simulation.

Raspberry Pi, which is a portable and cheap microcontroller, provides a powerful platform for designing and implementing management systems and control for MG applications through Python programming language, among other options. In this study, a Raspberry Pi 4b is employed for this purpose.

Finally, the PC host can locate MATLAB/Simulink and the RT-LAB software with the objective of performing their functions. Furthermore, it is used for the previous design and modelling of the system in Simulink.

This equipment permits to introduce the system to the experimental setup. The OPAL-RT 4512 unit locates the HMG and the local controllers through RT-LAB 2023.1 version. This model is built in Simulink previously in MATLAB 2022a. Otherwise, the centralized control, based on the EMS, is executed in the Raspberry Pi 4B microcontroller by using Python 3.7 programming language.

The HMG model is structured into three subsystems, allowing the real-time execution. In this regard, a master-subsystem includes the dynamic power model of the HMG, a slave-subsystem locates the control of the components of each MG. These subsystems are loaded into the OPAL-RT 4512 unit through the RT-LAB software. Finally, the last subsystem is the scope-subsystem, which is employed to visualize and monitor the response of the HMG and the control strategy.

3.2. Communication Link Protocol

OPAL-RT provides various communication protocols, which are employed for realistic real-time simulations in industry applications [15]. This fact allows for enhanced flexibility for user, without utilizing extra components.

TCP/UDP IO interface highlights between the various communication protocols offered by OPAL-RT. Among its characteristics emphasize versatility and an easy use. In this work, UDP is the communication protocol selected. UDP performs the data exchange among a client and a server [16].

The RT-LAB software and the Raspberry Pi microcontroller maintain real-time data exchange that occurs over an Ethernet network employing one IP address for the Raspberry Pi and another IP address for the OPAL-RT unit. For the correct connection of both equipment, the UDP port and the IP addresses must be configured on them and RJ45 cable for each equipment and a switch are employed

Additionally, the rate of the OPAL-RT unit is restricted by the decimation factor and the time step of the simulation, and the sleep time set in Phyton script marks the data exchange of the Raspberry Pi microcontroller. In this study the decimation factor is 500, the time step is 50 μs and the sleep time is 0 ms.

Hence, the communication process is realized as follow: the HMG sent to the EMS the generated energy by the PV generator and WT, the demanded energy by the loads and

the SOC of the BESSs from OPAL-RT. In the EMS, the active power references of the ESSs are obtained and, lastly, they are sent back to the HMG.

4 Experimental Results

In this section, to validate the effectiveness of the control strategy implemented in the HMG, a real-time experimental test was executed. As previously mentioned, the HMG and the local controllers were implemented and executed in an OPAL-RT 4512 unit, while the EMS was built in a Raspberry Pi microcontroller.

In this sense, a 10 s simulation was carried out under different conditions, as a variable wind speed and solar radiation and the connection and disconnection of the loads at different time intervals. These actions cause fluctuations in the generated and demanded energy.

Fig. 3 presents the active power exchange of all the ESSs in the HMG and their references. All the ESSs follow their active power references, demonstrating the effectiveness of the local controllers. Under conditions of excess electricity supply in the time intervals from 0 s to 0.5s and from 3 s to 4.2 s, the ESSs store energy. The remaining portion of the test, the generation is lower than the demand and the ESSs have to supply this deficit.

The SOC of the BESS is around 50% because it can be discharged and charged at the same rate as the hydrogen system, which supports the BESS. This action allows to extend the operation in the 'MEDIUM' range and reduce the SOC variation of the BESS.

Lastly, the UC fulfils its objective and contributes during transient power deviations, characterized by large power peaks and gradually diminishes its influence as the system stabilizes towards a steady state.

Fig. 4 depicts the electricity demand, the power generation, and the active power exchange with the main grid (P_{PCC}). The demanded energy varies depending on the disconnection and connection of the DC and AC loads to the MGs buses. In addition, the generated energy changes along the test depending on the variant wind speed and solar radiation.

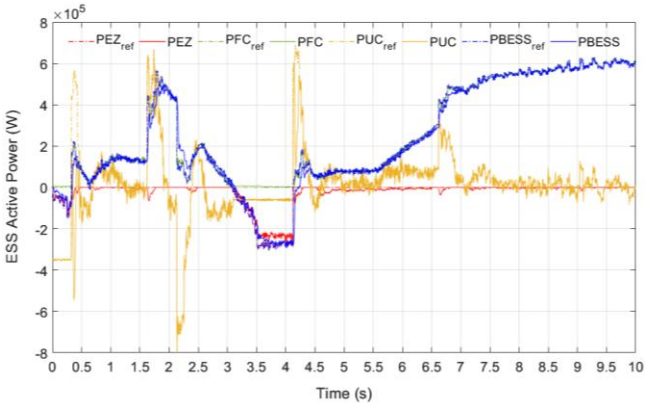

Fig. 3. Active power exchange of all the ESSs in the HMG.

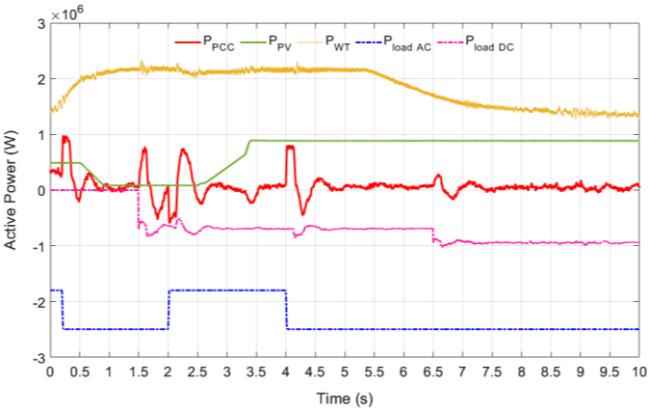

Fig. 4. The electricity demand, the power generation, and the active power exchange with the main grid (P_{PCC}).

All the loads are introduced as constant current values, but the DC loads exhibit slight power fluctuations in response to the DC bus voltage flicker. This effect is not observed on the AC loads because the main grid maintains a constant voltage on the AC bus.

Finally, the main grid actively participates in balancing power mismatches during changes in the HMG, either providing or absorbing the excess power that the ESSs cannot handle. When the power stability is reached, the power exchange with the main grid gradually diminishes and approaches zero.

The progression of the DC bus voltage is illustrated in Fig. 5. The results demonstrate that this parameter was precisely regulated around its target value of 1100 V. All the changes produced in the devices that compose the DC MG generate fluctuations on the voltage. Despite the disturbances, the DC voltage control loop implemented on the VSI of the DC MG effectively maintained the DC voltage around its reference

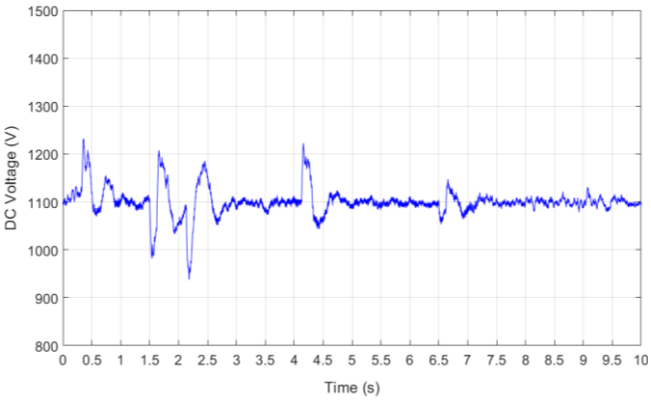

Fig. 5. DC bus voltage.

value. The precise regulation is essential for ensuring the stable operation of all components of this MG.

Hence, the results presented in this section provides evidence of the successful operation of the HMG, the local controllers, and the EMS implemented as centralized control.

5 Conclusions

This study developed a new control strategy for an HMG consisting of two MGs and a main grid. One of the MGs was an AC MG constituted by AC loads, a PV generator, and a battery bank. The other MG was a DC MG constituted by a hydrogen system, an UC, DC loads and WT. The DC MG was interconnected to the AC MG, and this last one, was connected to a three-phase main grid. The control strategy addressed a local control of each component of the MGs independently and a centralized control based on an EMS that managed the power in the HMG. For the validation of the results, an experimental setup was carried out, employing an OPAL-RT 4512 unit, a PC host, an oscilloscope, and a Raspberry Pi microcontroller. The OPAL-RT 4512 unit hosted the HMG, developed in MATLAB/Simulink and built in RT-LAB software, and the Raspberry Pi microcontroller hosted the EMS, programmed in Python. UDP was the communication protocol selected to execute the data exchange among the experimental setup equipment. The real-time system was tested under variable wind speed, solar radiation and loads, and the result obtained in this study presented a correct behaviour of the implemented control strategy.

Acknowledgements This work was partially supported by Ministerio de Ciencia e Innovación, Agencia Estatal de Investigación, FEDER, UE (Grant PID2021-123633OB-C32 supported by MCIN/AEI/10.13039/501100011033/ FEDER, UE).

References

1. B. Atilgan and A. Azapagic, “Life cycle environmental impacts of electricity from fossil fuels in Turkey,” J Clean Prod, vol. 106, pp. 555–564, 2014, doi: 10.1016/j.jclepro.2014.07.046.
2. A. Vasilakis, I. Zafeiratou, D. T. Lagos, and N. D. Hatziargyriou, “The Evolution of Research in Microgrids Control,” IEEE Open Access Journal of Power and Energy, vol. 7, pp. 331–343, 2020, doi: 10.1109/OAJPE.2020.3030348.
3. M. Shahbazitabar, H. Abdi, H. Nourianfar, A. Anvari-Moghaddam, B. Mohammadi-Ivatloo, and N. Hatziargyriou, “An Introduction to Microgrids, Concepts, Definition, and Classifications,” Power Systems, pp. 3–16, 2021, doi: 10.1007/978-3-030-59750-4_1.
4. L. de Oliveira-Assis et al., “Optimal energy management system using biogeography based optimization for grid-connected MVDC microgrid with photovoltaic, hydrogen system, electric vehicles and Z-source converters,” Energy Convers Manag, vol. 248, pp. 196–8904, 2021, doi: 10.1016/j.enconman.2021.114808.
5. S. K. Sahoo, A. K. Sinha, and N. K. Kishore, “Control Techniques in AC, DC, and Hybrid AC-DC Microgrid: A Review,” IEEE Journal of Emerging and Selected Topics in Power Electronics, vol. 6, no. 2. Institute of Electrical and Electronics Engineers Inc., pp. 738–759, Jun. 01, 2018. doi: 10.1109/JESTPE.2017.2786588.
6. C. Zhang, X. Yang, and J. Wang, “Survey on Isolated Microgrid Prognostics and Health Management,” 2022 2nd International Conference on Electrical Engineering and Control Science (IC2ECS), 2022, doi: 10.1109/IC2ECS57645.2022.10087926.
7. Y. Guan, J. C. Vasquez, and J. M. Guerrero, “Hierarchical Controlled Grid-Connected Microgrid based on a Novel Autonomous Current Sharing Controller,” 2015 IEEE Energy Conversion Congress and Exposition (ECCE), 2015, doi: 10.1109/ECCE.2015.7309988.
8. D. Ioris, A. B. De Almeida, and P. T. De Godoy, “A microgrid islanding performance study considering time delay in island detection,” 2020 IEEE PES Transmission and Distribution Conference and Exhibition - Latin America, T and D LA 2020, Sep. 2020, doi: 10.1109/TDLA47668.2020.9326168.
9. E. Unamuno and J. A. Barrena, “Hybrid ac/dc microgrids - Part I: Review and classification of topologies,” Renewable and Sustainable Energy Reviews, vol. 52. Elsevier Ltd, pp. 1251–1259, Aug. 22, 2015. doi: 10.1016/j.rser.2015.07.194.
10. M. Najafzadeh, R. Ahmadiahangar, O. Husev, I. Roasto, T. Jalakas, and A. Blinov, “Recent Contributions, Future Prospects and Limitations of Interlinking Converter Control in Hybrid AC/DC Microgrids,” IEEE Access, vol. 9, pp. 7960–7984, 2021, doi: 10.1109/ACCESS.2020.3049023.
11. T. Sattarpour, S. Golshannavaz, D. Nazarpour, and P. Siano, “A multi-stage linearized interactive operation model of smart distribution grid with residential microgrids,” International Journal of Electrical Power & Energy Systems, vol. 108, pp. 456–471, Jun. 2019, doi: 10.1016/J.IJEPES.2019.01.023.
12. S. Moussa and I. Slama-Belkhodja, “Residential loads modeling and load profile generation for microgrid EMS design in Tunisia,” 2022 IEEE International Conference on Electrical Sciences and Technologies in Maghreb, CISTEM 2022, 2022, doi: 10.1109/CISTEM55808.2022.10043983.
13. A. Yazdani and I. Reza, Voltage source converter in power system. 2010. Accessed: Jul. 28, 2023. [Online]. Available: https://www.wiley.com/en-ca/Voltage+Sourced+Converters+in+Power+Systems+%3A+Modeling%2C+Control%2C+and+Applications-p-9780470521564
14. M. A. Hasan and S. K. Parida, “An overview of solar photovoltaic panel modeling based on analytical and experimental viewpoint,” Renewable and Sustainable Energy Reviews, vol. 60, pp. 75–83, Jul. 2016, doi: 10.1016/J.RSER.2016.01.087.
15. “Real-Time Simulation Communication Protocols │ OPAL-RT,” 2022 - OPAL-RT TECHNOLOGIES, Inc. Accessed: Jul. 24, 2023. [Online]. Available: https://www.opal-rt.com/software-communication-protocols/
16. “TCP/UDP - OPAL-RT - Communication Protocol,” 2022 - OPAL-RT TECHNOLOGIES, Inc. Accessed: Jul. 24, 2023. [Online]. Available: https://www.opal-rt.com/software-communication-protocols/tcp-udp/#toggle-id-1